


Saikosaponin A Mediates the Anti-Acute Myeloid Leukemia Effect via the P-JNK Signaling Pathway Induced by Endoplasmic Reticulum Stress

Xiao-Hong Sun¹, Yi-Hong Chai¹, Xiao-Teng Bai¹, Hong-Xing Li¹, Pan-Pan Yang², Ya-Ming Xi^{1,3} 

¹The First Clinical Medical College of Lanzhou University, Lanzhou, 730000, People's Republic of China; ²Department of Gynecology and Obstetrics, The First Hospital of Lanzhou University, Lanzhou, 730000, People's Republic of China; ³Division of Hematology, The First Hospital of Lanzhou University, Lanzhou, 730000, People's Republic of China

Correspondence: Ya-Ming Xi, Division of Hematology, The First Hospital of Lanzhou University, Lanzhou, Gansu, People's Republic of China, Email xiyaming02@163.com

Objective: This study aims to investigate the antitumor effects of saikosaponin A (SSA) on acute myeloid leukemia (AML) and elucidate its underlying mechanisms, particularly focusing on the endoplasmic reticulum stress (ERS)-mediated MAPK-p-JNK signaling pathway.

Methods: The inhibitory effects of SSA on the proliferation of AML cell lines K562 and HL60 were evaluated using CCK8 and EdU assays. Apoptotic effects induced by SSA were analyzed via flow cytometry. RNA sequencing was performed to identify differentially expressed genes and enriched signaling pathways. Western blot analysis was utilized to confirm the involvement of ERS and activation of the MAPK-p-JNK signaling pathway. Further validation of the potential mechanism of SSA-induced apoptosis was conducted using SP600125 and 4PBA. The in vivo anti-AML efficacy of SSA was assessed using a xenograft model.

Results: SSA exhibited significant inhibitory effects on the proliferation of AML cell lines K562 and HL60, with IC₅₀ values at 12, 24, and 48 hours demonstrating time- and dose-dependency (19.84 μ M, 17.86 μ M, and 15.38 μ M for K562; 22.73 μ M, 17.02 μ M, and 15.25 μ M for HL60, respectively). Western blot analysis demonstrated that SSA induces apoptosis in AML cells through the mitochondrial apoptotic pathway. Transcriptomic profiling and Western blot analyses confirmed that SSA activates the ERS-mediated p-JNK signaling pathway to induce apoptosis in AML, a process that can be reversed by the addition of 4PBA or SP600125. Furthermore, SSA significantly reduced tumor volume and weight in a NOD-SCID mouse xenograft model without causing notable toxicity to the liver, kidneys, lungs, or heart, while also activating the ERS and p-JNK signaling pathways in vivo.

Conclusion: SSA induces apoptosis in AML cells by activating the ERS-mediated p-JNK signaling pathway, exhibiting significant anti-AML effects both in vitro and in vivo, accompanied by a favorable safety profile.

Keywords: saikosaponin A, acute myeloid leukemia, endoplasmic reticulum stress, JNK pathway, apoptosis

Introduction

AML represents the most prevalent form of acute hematologic malignancy in adults, characterized by genetic abnormalities within primitive hematopoietic stem cells (HSCs) and hematopoietic progenitor cells (HSPCs). These genetic alterations lead to unchecked proliferation and impaired differentiation of immature precursor cells within the bone marrow.¹ Over recent decades, the standard treatment modality for AML has predominantly consisted of intensive chemotherapy, commonly utilizing the “3+7” regimen, which combines anthracyclines with cytarabine for induction therapy. This initial treatment phase is frequently followed by multiple cycles of consolidation chemotherapy or consideration for hematopoietic stem cell transplantation.² Nevertheless, the toxic side effects associated with anthracyclines and cytarabine present considerable challenges for patients, adversely impacting their quality of life and treatment adherence.³ Consequently, there is a pressing imperative to investigate and develop low-toxicity therapeutic agents that can enhance clinical outcomes for individuals diagnosed with AML.

In recent years, natural products from plants, fruits and other food sources have been increasingly used in the field of tumor therapy.^{4,5} A study has shown that a water-soluble extract of the traditional Chinese medicine Chai Hu was shown to attenuate DNA damage caused by 5-fluorouracil in the hepatocellular carcinoma cell line HepG2 and to promote apoptosis through activation of mitochondria-mediated apoptotic mechanisms, without causing damage to normal human lymphocytes.⁶ This suggests that the active ingredient of SSA possesses significant antitumor properties and is well compatible with noncancerous cells. SSA is a triterpenoid saponin extracted from the medicinal plant *Saikosaponinum falciparum* and is known for its wide range of pharmacological activities including anti-inflammatory, antitumor, antifibrotic, and antidepressant effects, as well as immune function enhancement.⁷ There is growing evidence that SSA possesses significant anticancer effects with low toxicity, and has been shown to be effective in inhibiting the growth of a wide range of cancers (hepatocellular carcinoma, gastric cancer, breast cancer, and prostate cancer).^{8–11} However, the effect of SSA on AML is still unclear.

ERS arises from a variety of physiological and pathological factors, disrupting the homeostatic balance of the endoplasmic reticulum (ER) and resulting in the accumulation of unfolded or misfolded proteins within the ER lumen. As a cellular defense mechanism, ERS engages the unfolded protein response (UPR) to maintain cellular integrity and alleviate the burden posed by abnormal protein accumulation. However, if ERS is prolonged or intensively activated, it can initiate apoptotic pathways and trigger immune responses, ultimately impairing cell survival.¹² In antitumor therapeutic strategies, ERS can be harnessed in two primary ways: first, by inhibiting UPR-mediated cell survival signaling to reduce tumor cell adaptation; and second, by inducing sustained ERS, which activates pro-apoptotic signaling pathways that drive tumor cell apoptosis. During ERS, the activation of the Protein kinase RNA-like endoplasmic reticulum kinase (PERK) pathway plays a critical role in regulating protein synthesis by phosphorylating Eukaryotic initiation factor 2 alpha (eIF2 α), thereby reducing the load on the endoplasmic reticulum. However, in the context of excessive or prolonged ERS, the PERK/eIF2 α signaling pathway not only decreases protein synthesis but also activates c-Jun N-terminal kinase (JNK), subsequently triggering apoptotic pathways. This highlights the dual role of ERS in determining cellular fate.¹³ Previous studies have demonstrated that ERS mediates the JNK/p38 Mitogen-Activated Protein Kinase (MAPK) signaling pathway in hepatocellular carcinoma cells, leading to cell death.¹⁴ Additionally, given that SSA has shown potential in mediating the ERS pathway to induce apoptosis in tumor cells,^{8, 15, 16} the potential mechanism of its treatment of AML deserves to be investigated.

Therefore, this study aims to systematically investigate how SSA affects the phosphorylation of c-Jun N-terminal kinase (P-JNK) signaling pathway by inducing ERS, which contributes to its therapeutic effects on AML. The ultimate goal of this study is to provide a novel theoretical framework and therapeutic strategy for the treatment of AML, as well as to enhance the potential of natural compounds in cancer therapy.

Materials and Methods

Cell Culture

K562 and HL60 cell lines were procured from the Laboratory of Clinical Molecular Cytogenetics and Immunology, the first hospital of Lanzhou University. The GES-1, HK-2, and SV-HUC-1 cell lines, which were purchased from Servicebio (Cat. No. STCC10303P, STCC12301P, and STCC10401P, respectively). K562, HL60 and GES-1 cells were cultured in RPMI-1640 (BasalMedia) medium supplemented with 10% fetal bovine serum (Excell Bio) and 1% penicillin-streptomycin (Excell Bio). HK-2 cells are cultured using a specialized HK-2 cell culture medium (Servicebio, GZ10303). SV-HUC-1 cells are cultured using a specialized SV-HUC-1 cell culture medium (Servicebio, GZ12301). The cells were maintained in an incubator (BIOBASE) set at 37°C with 5% CO₂ and 95% humidity. For subsequent experiments, cells in the logarithmic phase of growth were utilized.

Cell Viability Assay

SSA (purity > 99%, MCE) was dissolved in dimethyl sulfoxide (DMSO) and further diluted to prepare a 10 mm master mix using complete culture medium, which was stored at –80°C. K562 and HL60 cells were seeded in 96-well plates (JETBIOFIL) at densities of 1 x 10⁴ and 2 x 10⁴ cells per well, respectively, and subjected to SSA

treatment at concentrations of 10, 20, 30, 40, and 50 μM . We seeded GES-1, HK-2, and SV-HUC-1 cells at a density of 2000 cells per well in 96-well plates and treated them with 0, 8, 12, 16, and 32 μM SSA. Following a treatment period of 12, 24, and 48 hours, 10 μL of Cell Counting Kit 8 reagent (CCK8, Beyotime) was added to each well. After 1.5–3 hours of incubation at 37°C, absorbance was measured at 450 nm using a multifunctional enzyme-labeled reader (Thermo Fisher Scientific) to assess optical density. Subsequent experiments aimed to evaluate the impact of varying concentrations of SSA on cell viability, focusing on the determination of IC50 values (n=9).

EDU Assay

Cell proliferation was assessed using the EdU method with the Cell Proliferation Imaging Analysis Kit (Abbkine). Following drug treatment, cells were inoculated into a 96-well plate and subsequently incubated with EdU (10 μM) for 2 hours. After incubation, the cells were centrifuged, fixed, and washed thoroughly. The cells were then incubated with PBS containing 0.5% Triton X-100 for 15 minutes, followed by centrifugation and washing. The Click-iT reaction mixture was applied for 30 minutes at room temperature, protected from light. After repeating the washing steps, nuclei were stained with Hoechst 33342 for 10 minutes. Finally, images were captured using a fluorescence microscope (Leica) (n=5).

Isolation and Cell Viability Assay of Human Bone Marrow Mononuclear Cells

Bone marrow samples were obtained from patients diagnosed with incipient AML, and bone marrow mononuclear cells (BMMCs) were isolated through density gradient centrifugation. The fresh bone marrow aspirate was carefully transferred into a sterile centrifuge tube containing 3–4 mL of lymphocyte isolation solution (Solarbio) and centrifuged at 2000 rpm for 25 minutes. This process yielded four distinct layers: the plasma layer, a milky-white ring of mononuclear cells, a clear separating solution layer, and an erythrocyte layer. The milky-white mononuclear cell layer was subsequently collected into a new sterile centrifuge tube, washed with PBS, and further centrifuged at 1500 rpm for 10 minutes, with this washing step repeated twice. Erythrocytes present in the pellet were removed with erythrocyte lysis buffer, resulting in the isolation of pure bone marrow mononuclear cells. The final yield of bone marrow mononuclear cells was resuspended in complete medium composed of RPMI-1640 supplemented with 20% fetal bovine serum (FBS) and 1% penicillin-streptomycin, and the cells were incubated in the incubator for 1 day to ensure optimal viability of the bone marrow progenitor cells. Subsequently, the cells were plated in 96-well plates at densities of 80–120 $\times 10^4$ cells per well. The viability of the cells was assessed using the CCK8 assay following a 24-hour treatment period with different concentrations of SSA (10, 20, 30, 40, and 50 μM). For detailed procedures, refer to [Supplementary Method 1](#). The study received approval from the Research Ethics Committee of the First Hospital of Lanzhou University (approval number: LDYYLL2024-485), all participants provided signed written informed consent prior to their inclusion in the study. Basic Characteristics about AML patients is shown in [Table S1](#).

Apoptosis Assay

Following treatment with SSA at concentrations of 8, 12, and 16 μM for 24 hours, apoptosis was evaluated using the Annexin V-FITC/PI apoptosis kit (MULTI SCIENCES). The treated cells were collected, and 5 μL of Annexin V-FITC and 10 μL of propidium iodide (PI) were added to the cell suspension. The mixture was incubated for 5 minutes at room temperature, shielded from light. Stained cells were subsequently analyzed using flow cytometry (Agilent Technologies, NovoCyte Advanteon Dx VBR) (n=5).

Cell Cycle Analysis

The collection of treated cells was performed as described previously, and cell cycle distribution was assessed using the Cell Cycle Assay Kit (MULTI SCIENCES). A volume of 1 mL of DNA staining solution combined with 10 μL of propidium iodide (PI) solution was incubated for 30 minutes at room temperature, away from light. The stained cells were then analyzed via flow cytometry (Agilent Technologies) (n=5).

Mitochondrial Membrane Potential Detection

Treated cells were collected in a manner consistent with previous protocols, and alterations in mitochondrial membrane potential (MMP) were measured using the Mitochondria Staining Kit (MULTI SCIENCES). The collected cells were resuspended in 2 μ M JC-1 solution and incubated in an incubator for 20 minutes. Following incubation, the cells were washed once with warm PBS and resuspended for analysis. The detection was conducted using a flow cytometer with excitation at 488 nm, capturing data through FITC and R-PE channels (n=5).

Transcriptome Sequencing Data Mining

HL60 cells were treated with 0, 14 μ M SSA for 24 hours respectively (n=6). After treatment, cells were collected and fixed in RNAiso Plus (TakaRa). The samples underwent RNA sequencing facilitated by Frasergen Bioinformatics on the DNBSEQ-T7 Sequencing Platform. Differentially expressed genes were analyzed for Kyoto Encyclopedia of Genes and Genomes¹⁷ (KEGG) pathway and Gene Set Enrichment Analysis¹⁸ (GSEA) enrichment. See [Supplementary Method 2](#) for comprehensive operational details.

Western Blot Analysis

Cells were lysed using RIPA lysis buffer (Beyotime, medium potency), which contained inhibitors for protease and protein phosphatase, to extract total cellular proteins. Cytoplasmic proteins were extracted subsequently using the Cytoplasmic Protein Extraction Kit (Beyotime), with protein concentration determined using the BCA kit (Epizyme Biotech). Fifteen to twenty micrograms of protein were subjected to electrophoresis on a 10% SDS-PAGE gel (NCM Biotechnology, China), following which the proteins were transferred to a PVDF membrane (Millipore). Membranes were blocked with 5% skimmed milk powder and incubated overnight at 4°C with the primary antibody. Following this, membranes were washed with Tris-buffered saline containing Tween-20 and incubated with secondary antibodies (Proteintech, SA0001-2) for 1 hour at room temperature. Signal detection was performed using Enhanced Chemiluminescence Fluorescence Chromogenic Solution (Epizyme Biotech), and images were captured using a chemiluminescence imaging system (Amersham Imager 680). The primary antibodies used in this study are detailed in [Table 1](#).

Tumor Xenograft Assay

NOD-SCID mice (4 weeks old, female) were procured from Huachuang Sino Pharmaceutical Technology Co. All animal experiments were conducted in accordance with the regulations set forth by the Ethics Committee of the First Hospital of

Table 1 Primary Antibodies Used in Western Blotting

Antibody	Company	Cat No.
Bax	Proteintech	50599-2-Ig
Bcl-2	Proteintech	26593-1-AP
cytc	Abmart	T55994S
Cleaved caspase3	abcolony	A11201
Pp38	Immunoway	YP0338
P38	Immunoway	YT3513
JNK1/2/3	Immunoway	YT2440
p-JNK	Immunoway	YP0157
ERK 1/2	Immunoway	YT1625
p-erk	Immunoway	YP0101
p-PERK	MedChemExpress	HY-P80845
PERK	MedChemExpress	HY-p80781
Bip	Affinity	AF5366
Chop	Affinity	AF6277
GAPDH	BOSTER	BST23373874
TuBB1	BOSTER	23XB3530C16

Lanzhou University (Grant No. LDYYLL2024-485). The mice were maintained under specific-pathogen-free conditions with controlled temperature and humidity. Following a one-week acclimatization period, the mice were randomly divided into two groups: the K562 group (n=10) and the HL60 group (n=15). K562 (5×10^6) and HL60 (5×10^6) cells, which were in the logarithmic growth phase, were injected into the right anterior axilla of the corresponding groups of mice to establish xenograft tumor models. Upon the appearance of visible tumors, tumor size measurements were taken every other day, with the volume calculated using the formula $(\text{length} \times \text{width}^2)/2$. Additionally, the body weight of the mice was monitored throughout the study. Once the tumor volume reached approximately 100 mm³, the K562 group was randomly subdivided into two subgroups (n=5), one receiving intraperitoneal injections of SSA (7.5 mg/kg) and the other receiving an equal volume of the SSA solvent every other day. The HL60 group was divided into three subgroups (n=5): a low-dose SSA group (5 mg/kg), a high-dose SSA group (7.5 mg/kg), and a control group receiving an equal volume of the SSA solvent (50% PEG300 and 50% saline). The treatment regimen continued for three weeks. At the conclusion of the experimental period, the mice were euthanized, and the livers, kidneys, hearts, and lungs were meticulously dissected. These organs were rapidly fixed in 4% paraformaldehyde, and paraffin-embedded sections were prepared for hematoxylin and eosin (HE) staining to evaluate the potential toxic effects of SSA on standard organ systems (n=5).

Statistical Analysis

Data were analyzed using GraphPad Prism software (version 9.0), with comparisons between groups conducted utilizing independent samples *t*-test or one-way ANOVA for single-group comparisons. For assessments involving multiple groups, two-way ANOVA was employed. Results are presented as means \pm standard deviation. All experiments were repeated three times to ensure reproducibility. Significant differences were considered at *p*-values less than 0.05, with the following notations for significance levels: [#]*p* < 0.0001, ****p* < 0.001, ***p* < 0.01, **p* < 0.05, ^{ns}*p* > 0.05.

Results

Effect of SSA on AML Cell Lines and BMNCs Activity

The chemical structure of SSA is depicted in [Figure 1A](#). To quantitatively assess the effect of SSA on the proliferation of AML cell lines K562 and HL60 at varying concentrations of SSA, we performed the CCK8 cell proliferation assay to evaluate cell viability. The results, as shown in [Figure 1B](#), indicate that SSA significantly inhibited the proliferation of AML cells. The calculated IC₅₀ values for K562 and HL60 cells at time points of 12, 24, and 48 hours were 19.84 μM and 22.73 μM, 17.86 μM and 17.02 μM, and 15.38 μM and 15.25 μM, respectively. This inhibitory effect demonstrated both concentration- and time-dependent characteristics, with the K562 cell line exhibiting greater sensitivity to SSA compared to the HL60 cell line. Based on the findings from the CCK8 assay, cells treated with SSA for 24 hours at concentrations of 8, 12, and 16 μM were selected for further in vitro studies. Additional analysis utilizing the EDU proliferation assay revealed a significant reduction in the proportion of EDU-positive cells corresponding to increasing SSA concentrations ([Figure 1C](#)), as illustrated in [Table 2](#).

To further validate the cytotoxic effect of SSA on AML cells, we collected specimens from patients diagnosed with primary AML. Our findings demonstrated that SSA also markedly inhibited the viability of primary leukemia cells, although the magnitude of the inhibitory effects varied among patients. However, the IC₅₀ values were consistently below 40 μM ([Figure 1D](#)).

Additionally, to demonstrate that SSA can inhibit AML cell proliferation without causing toxicity to normal epithelial cells, we performed CCK8 assays using three types of epithelial cells: GES-1, HK-2, and SV-HUC-1. The results showed no significant inhibition of proliferation in these epithelial cells after treatment with SSA at concentrations of 8, 12, 16, and 32 μM for 12, 24, and 48 hours ([Figure 1E](#)). This indicates that SSA selectively inhibits AML cells while showing minimal toxicity to normal epithelial cells. Through these experiments, we have confirmed the effective inhibitory effect of SSA on AML cells and its potential therapeutic value, while also demonstrating its safety for normal epithelial cells.

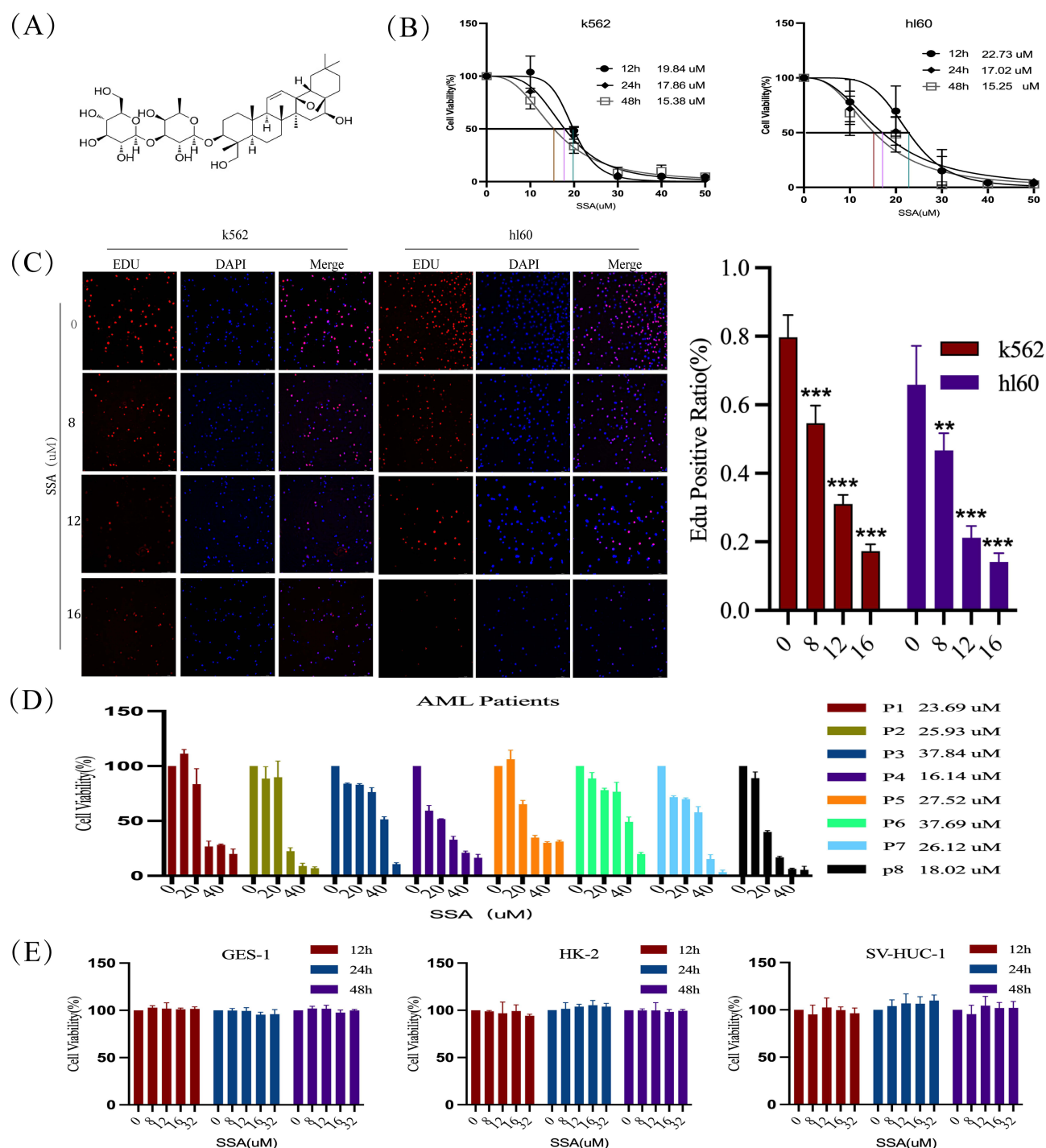


Figure 1 Effect of SSA on cell proliferation. (A) Chemical structure of SSA. (B) Cell viability of K562 and HL60 after treatment with SSA (0–50 μM) for 12, 24, and 48 hours, assessed by CCK8 assay (K562/12h: $19.84 \pm 0.94 \mu\text{M}$, 24h: $17.86 \pm 0.88 \mu\text{M}$, 48h: $15.38 \pm 0.77 \mu\text{M}$, HL60/12h: $22.73 \pm 1.34 \mu\text{M}$, 24h: $17.02 \pm 1.91 \mu\text{M}$, 48h: $15.25 \pm 1.75 \mu\text{M}$) ($n=9$). (C) Proportion of EDU-positive AML cells after 24-hour treatment with SSA (8, 12, and 16 μM) ($n=5$). (D) Viability of human acute myeloid leukemia progenitor cells after 24-hour treatment with SSA (0–50 μM), as determined by CCK8 assay ($n=8$). (E) Cell viability of GES-1, HK-2, and SV-HUC-1 after treatment with SSA (8, 12, 16 and 32 μM) for 12, 24, and 48 hours, assessed by CCK8 assay ($n=9$, $p > 0.05$). Significance is denoted as $**p < 0.01$, $***p < 0.001$. The analysis was performed using GraphPad Prism software (version 9.0).

SSA Induces Apoptosis in AML Cells

To evaluate whether SSA inhibits the proliferation of AML cells through the promotion of apoptosis, we analyzed the apoptotic effects of SSA on K562 and HL60 cells by flow cytometry following exposure to different concentrations of SSA (8, 12, and 16 μM). The experimental results demonstrated that SSA significantly enhanced the apoptotic process in both K562 and HL60

Table 2 Proportion of EDU-Positive AML Cells After 24-Hour Treatment with SSA (μM)

	0	8	12	16
K562	79.7% \pm 6.5%	54.7% \pm 5.1%***	31% \pm 2.7%***	17.3% \pm 2%***
HL60	66% \pm 11.4%	47% \pm 5%*	21% \pm 3.4%***	14% \pm 2.5%***

Note: Mean \pm SD, **p < 0.01, ***p < 0.001 compared to control group.

cells, with this effect exhibiting a concentration-dependent characteristic. Specifically, higher concentrations of SSA corresponded to markedly increased apoptotic rates (Figure 2A). Notably, at a concentration of 16 μM , the apoptosis rate for K562 cells reached 67.4%, while HL60 cells displayed an apoptosis rate of 55.61%. Further analysis revealed that both early and late apoptotic cell populations exhibited a significant dose-dependent increase following SSA treatment ($p < 0.05$). Additionally, investigations into the underlying molecular mechanisms indicated that SSA treatment upregulated the expression of the pro-apoptotic protein Bax while simultaneously downregulating the expression of the anti-apoptotic protein Bcl-2. This shift was accompanied by the activation of caspase-3 (Figure 2B). Collectively, these findings substantiate the conclusion that SSA induces apoptosis in AML cells, with the magnitude of this effect being accentuated by increasing SSA concentrations.

SSA Decreases Mitochondrial Membrane Potential in AML Cells

Dynamic alterations in mitochondrial membrane potential (MMP) serve as critical indicators of mitochondrial dysfunction during the early stages of apoptosis. To further investigate the role of SSA in inducing apoptosis, we assessed the

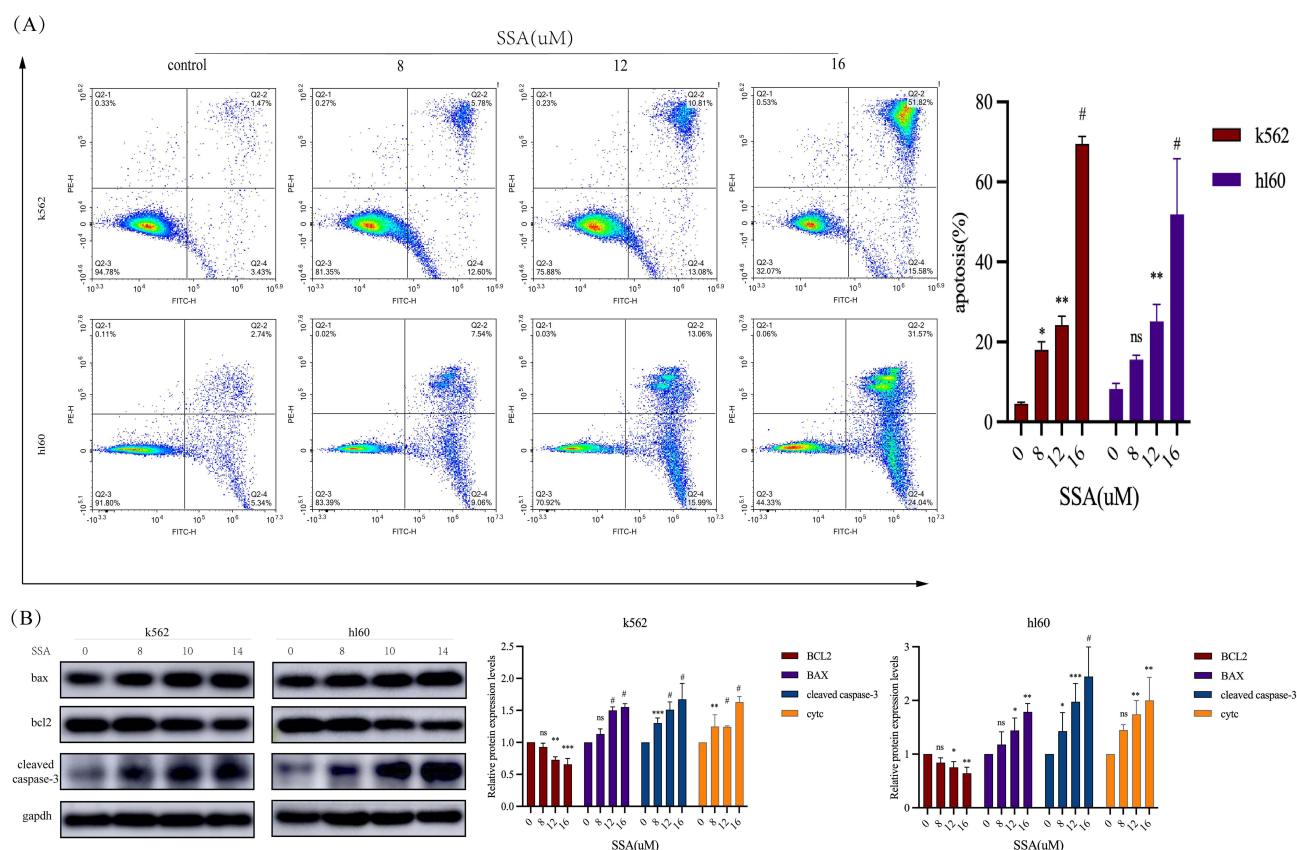


Figure 2 Effect of SSA on AML apoptosis. **(A)** Apoptosis promotion and statistical analysis of AML cells after 24-hour treatment with SSA (Rate of apoptosis in K562/0: 4.59% \pm 0.28%, 8 μM : 18.04% \pm 1.98%, 12 μM : 24.25% \pm 2.17%, and 16 μM : 67.4% \pm 1.87%, HL60/0: 8.17% \pm 1.4%, 8 μM : 15.51% \pm 1.03%, 12 μM : 25.11% \pm 4.17%, and 16 μM : 55.61% \pm 13.87%) (n=5). **(B)** Effects and statistical analysis of SSA (8, 12, and 16 μM) on the expression of apoptosis-related proteins BAX, cleaved-caspase-3, and Bcl2 after 24 hours, with GAPDH as a loading control (n=5). Significance is denoted as *p < 0.05, **p < 0.01, ***p < 0.001, #p < 0.0001, ns p > 0.05. The analysis was performed using GraphPad Prism software (version 9.0).

changes in MMP following a 24-hour exposure to SSA in AML cells using flow cytometry. The results demonstrated that treatment with SSA led to a concentration-dependent reduction in MMP (Figure 3A).

Furthermore, our findings revealed that SSA facilitated the release of cytochrome C from the mitochondrial inner membrane into the cytoplasmic matrix of AML cells. This release represents a pivotal event in the apoptotic process and signifies the initiation of the apoptotic execution phase (Figure 3B). Collectively, these results indicate that SSA promotes the release of cytochrome C from mitochondria into the cytosol by inducing a decline in MMP, consequently activating a downstream cascade of events that ultimately advances apoptosis in K562 and HL60 cells.

SSA Induces Cell Cycle Arrest in AML

Cell proliferation is intricately regulated by the cell cycle. To evaluate the impact of SSA on the cell cycle progression of AML cells, K562 and HL60 cells treated with SSA were stained with PI and analyzed using flow cytometry. The results demonstrated that SSA treatment predominantly arrested these cell lines in the S-phase of the cell cycle, concomitant with a notable reduction in the proportion of cells in the G2/M phase. Our results suggest that SSA also inhibits proliferation by inducing K562, HL60 cell cycle S phase arrest to inhibit proliferation (Figure 4). We have also represented the proportions of cells in different phases of the cell cycle and their statistical significance in Table 3.

Transcriptome Sequencing Reveals the Effect of SSA on the MAPK Signaling Pathway

To further explore the potential mechanisms of SSA action in AML, SSA-treated HL60 cells were subjected to a comprehensive transcriptome analysis. Specifically, by assessing differential gene expression between control and

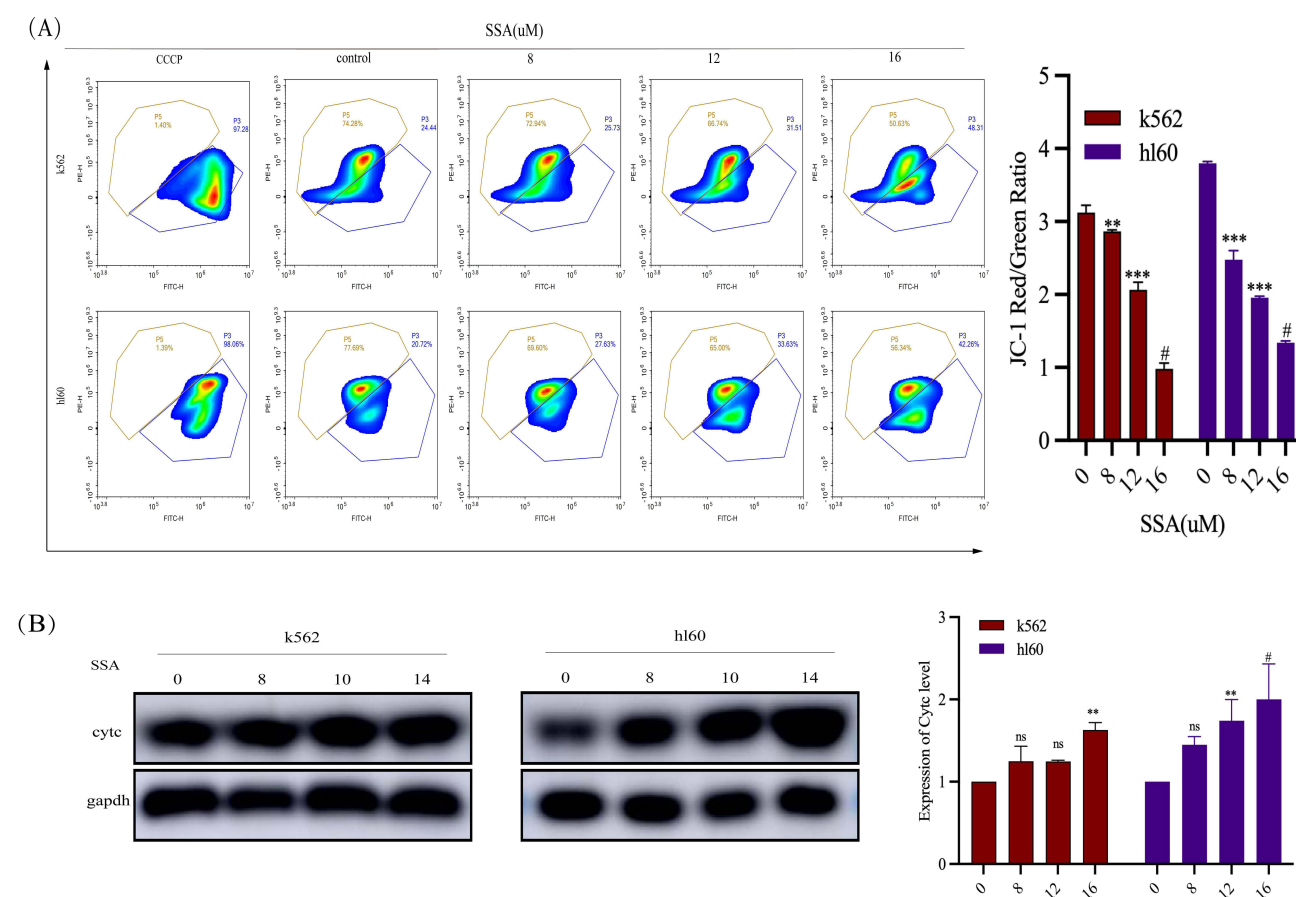


Figure 3 SSA reduces MMP in AML cells. **(A)** SSA (8, 12, 16 μM) significantly decreased the mitochondrial membrane potential of AML cells after 24 hours (n=5). **(B)** Increased levels of cytochrome C in the cytoplasm of AML cells 24 hours after SSA (8, 12, 16 μM) treatment, with GAPDH as a loading control (n=5). Significance is denoted as **p < 0.01, ***p < 0.001, #p < 0.0001, ns p > 0.05. The analysis was performed using GraphPad Prism software (version 9.0).

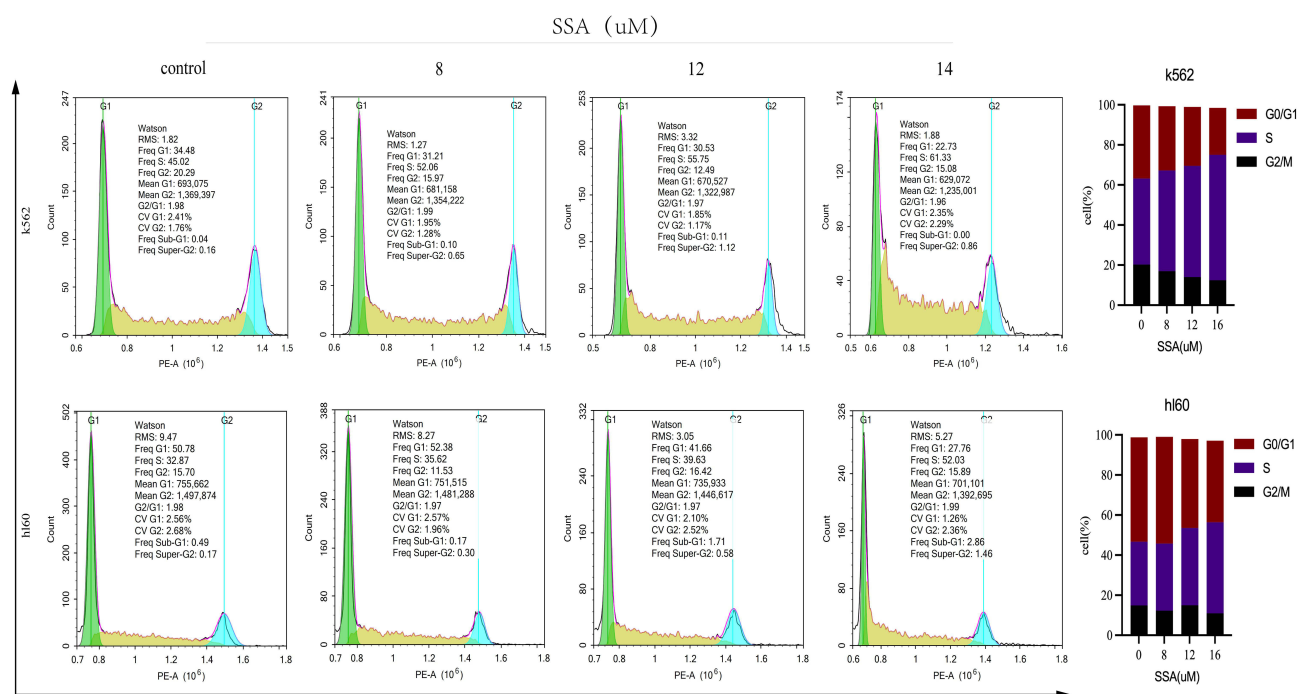


Figure 4 SSA arrested K562, HL60 cell cycle progression at the S phase (n=5).

SSA treatment, the analysis yielded 306 up-regulated genes and 52 down-regulated genes ($|\log_2$ fold change >1 , $p < 0.05$), as shown in Figure 5A. The differentially expressed genes were analyzed by KEGG enrichment analysis to highlight the key pathways, especially in the NF-kappa B signaling pathway, TNF signaling pathway, and MAPK signaling pathway, which are closely related to tumor progression, while the enrichment of MAPK signaling pathway was the most significant (Figure 5B). GSEA further confirmed that the MAPK signaling pathway was significantly enriched after SSA treatment of HL60 cells (Figure 5C), and the data from transcriptome sequencing suggested that SSA may exert its anti-AML effect through mediating the MAPK signaling pathway.

SSA Activates the MAPK Signaling Pathway and Mediates ERS

To further elucidate the mechanism by which SSA promotes apoptosis in AML cells, we investigated its effect on the MAPK signaling pathway using Western Blotting to assess the expression levels of phosphorylated Extracellular Signal-Regulated Kinase (p-ERK/ERK), JNK (p-JNK/JNK), and p38 (p-P38/P38). Following a 24-hour treatment with SSA, we observed a dose-dependent increase in the phosphorylation levels of JNK in both HL60 and K562 cells. As the SSA concentration increased, there was a significant upregulation of the relative expression of key proteins, specifically p-JNK/JNK and p-P38/P38, while no notable changes were observed in the expression of p-ERK/ERK (Figure 6A).

Table 3 Effect of a 24-Hour SSA Treatment on the Cell Cycle Distribution in K562 and HL-60 Leukemia Cell Lines (%)

SSA (uM)	0	8	12	16
K562 G2/M	20.3±1.92	16.92±1.1 ^{ns}	14.07±1.43*	12.47±2.89**
K562 S	42.94±2.4	50.32±2.58 ^{ns}	55.51±1.68**	62.61±4.94***
K562 G0/G1	36.45±3.77	32.05±3.01 ^{ns}	29.38±2.21 ^{ns}	23.34±6.59*
HL60 G2/M	14.89±0.912	12.29±2.48 ^{ns}	14.99±2.14 ^{ns}	10.97±5.46 ^{ns}
HL60 S	31.8±1.06	33.49±2.05 ^{ns}	38.59±1.16 ^{ns}	45.44±6.02**
HL60 G0/G1	52.08±1.15	53.27±2.72 ^{ns}	44.4±2.46 ^{ns}	40.74±12.62 ^{ns}

Note: Mean ± SD, ^{ns} $p > 0.05$, * $p < 0.05$, ** $p < 0.01$, *** $p < 0.001$ compared to control group.

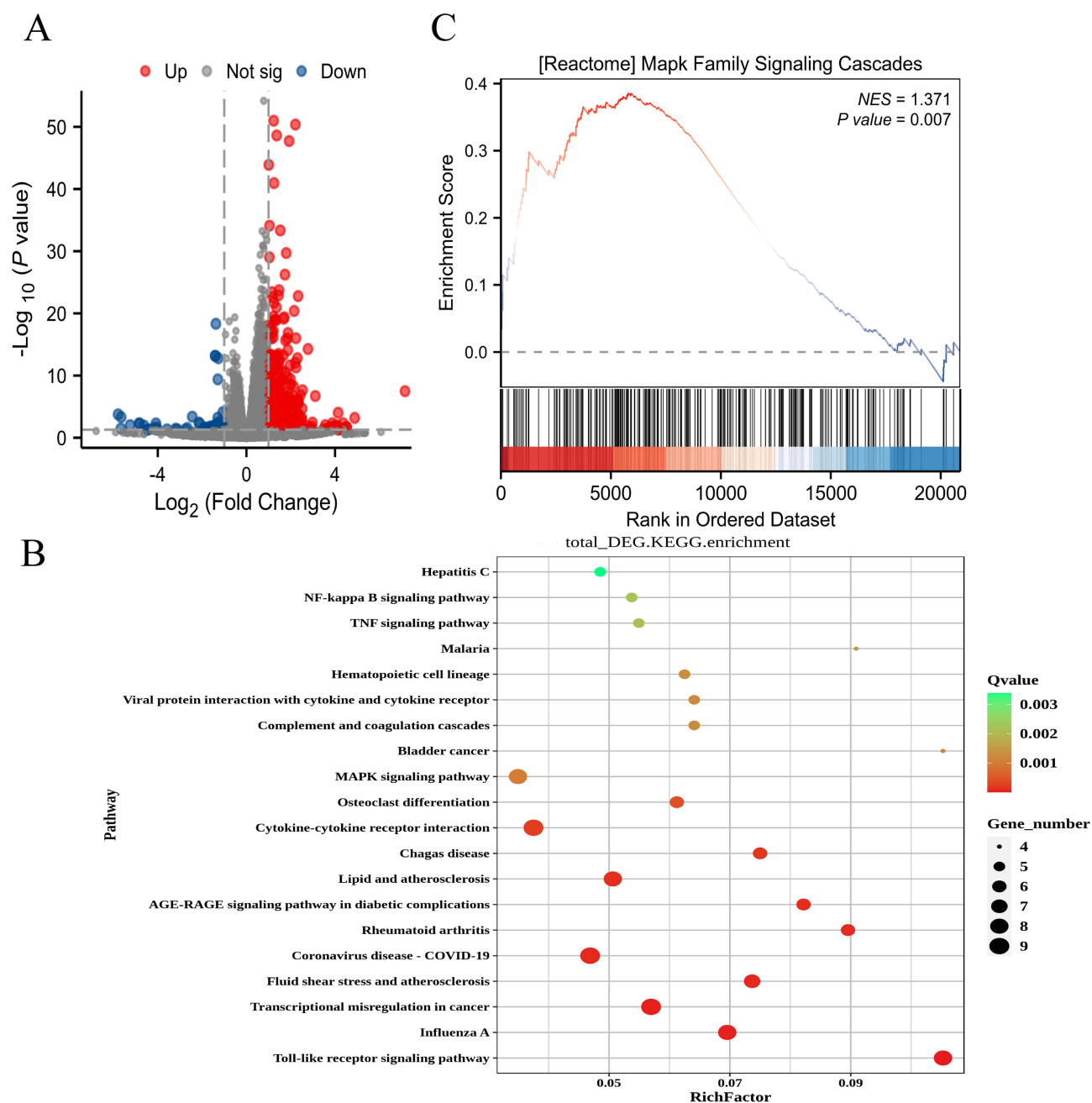


Figure 5 SSA regulates the MAPK signaling pathway in acute myeloid leukemia (n=6). **(A)** Volcano plots showing up- and down-regulated differential genes in HL60 cells after 24 h of SSA treatment ($|\log_2 \text{Fold Change}| > 1$, $p < 0.05$). **(B)** KEGG pathway enrichment analysis identifying the top 20 pathways significantly associated with SSA treatment. **(C)** GSEA demonstrating significant enrichment in the MAPK signaling pathway post SSA treatment, indicated by $NES > 1$ and $p < 0.05$.

Notably, the most pronounced increase was recorded in the expression levels of p-JNK/JNK in response to escalating doses of SSA. Given that endoplasmic reticulum (ER) stress can activate the JNK signaling pathway via multiple mechanisms, we further explored the impact of SSA on ER stress in HL60 and K562 cells. The expression levels of ER stress-related marker proteins were evaluated using Western Blotting. Our findings indicated that SSA significantly upregulated the protein expression levels of ER stress markers, including Phosphorylated PKR-like ER Kinase (p-PERK/PERK), Binding Immunoglobulin Protein (Bip), and C/EBP Homologous Protein (CHOP), in a dose-dependent manner (Figure 6B).

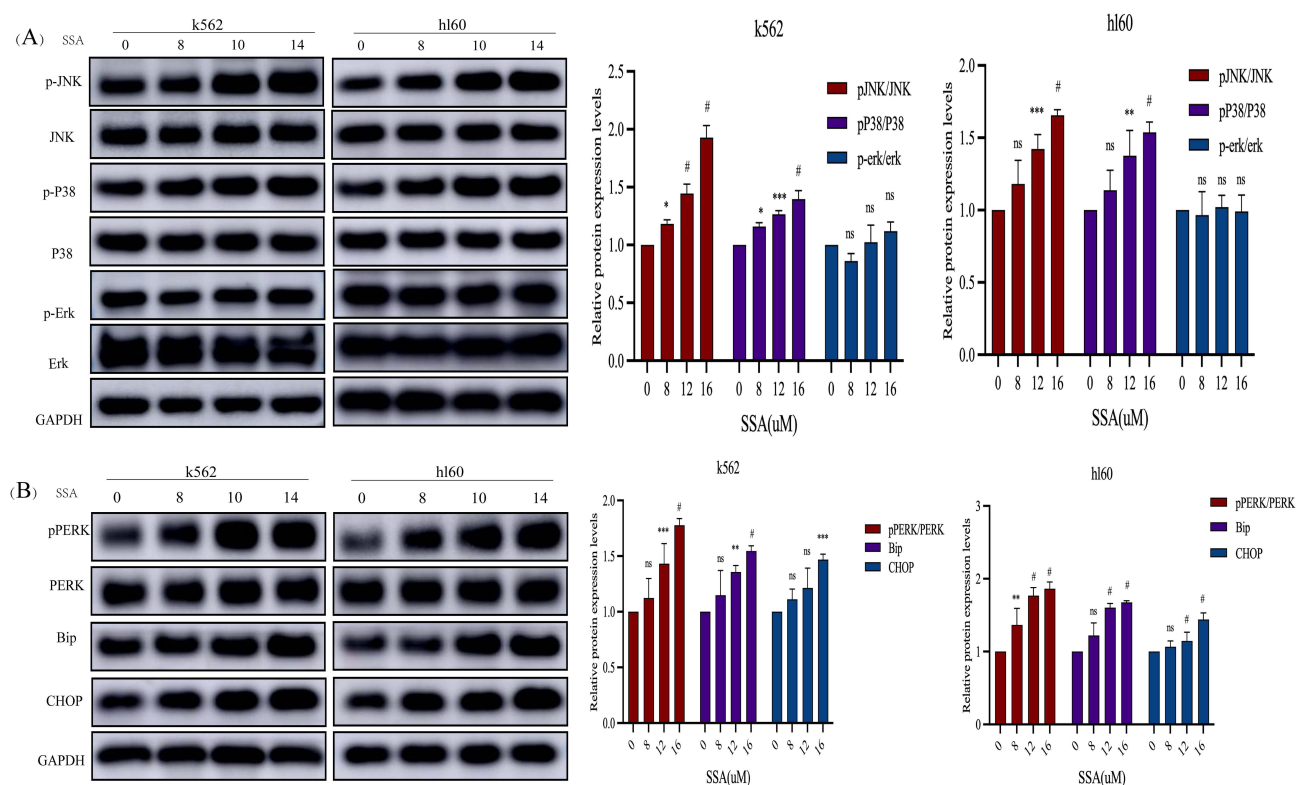


Figure 6 SSA activates the MAPK signaling pathway and mediates ERS (n=5). **(A)** Western blot analysis of protein expression levels of p-JNK/JNK, p-P38/P38, and p-ERK/ERK in AML cells following 24 hours of treatment with SSA (8, 12, 14 μM). GAPDH served as a loading control. **(B)** Western blot analysis of ER stress markers p-PERK/PERK, Bip, and CHOP in AML cells after 24 hours of SSA (8, 12, 14 μM) treatment. GAPDH served as a loading control. Significance is denoted as *p < 0.05, **p < 0.01, ***p < 0.001, #p < 0.0001, ^{ns}p > 0.05. The analysis was performed using GraphPad Prism software (version 9.0).

These results suggest that SSA induces apoptosis in AML cells through the activation of the MAPK-p-JNK/p38 signaling pathway, which is mediated by ER stress.

SSA Induces Apoptosis Through the MAPK-p-JNK Signaling Pathway

To investigate whether SSA-induced apoptosis is mediated by the MAPK-p-JNK signaling pathway, we employed the JNK-specific inhibitor SP600125 in our subsequent experiments. Flow cytometric analysis revealed that SP600125 effectively prevented SSA-induced apoptotic progression in AML cells, without exhibiting significant effects on basal AML cell apoptosis (**Figure 7A**). Western blot analysis demonstrated that SP600125 significantly inhibited the activation of the p-JNK/JNK signaling pathway caused by SSA in AML cells (**Figure 7B**). Furthermore, treatment with SP600125 resulted in a reduction in the levels of pro-apoptotic proteins, including Bax and cleaved caspase-3, alongside an increase in the expression of the anti-apoptotic protein Bcl-2. This suggests that SP600125 partially reverses the alterations in apoptosis-related protein expression induced by SSA (**Figure 7C**). In summary, these findings indicate that SSA induces apoptosis in AML cells through the activation of the JNK signaling pathway. This research enhances our understanding of the mechanisms underlying the anti-leukemic effects of SSA and provides a theoretical framework for developing AML therapeutic strategies targeting the regulation of the JNK signaling pathway.

SSA Induces Apoptosis Through the ERS-Mediated p-JNK Signaling Pathway

A close relationship exists between ERS and the JNK signaling pathway. To further verify whether apoptosis induced by the SSA-activated p-JNK signaling pathway is mediated through ERS, K562 and HL60 cells were treated with the ERS inhibitor 4-phenylbutyric acid (4-PBA) alone or in combination with SSA for 24 hours. Apoptosis was assessed through flow cytometric analysis, revealing that while 4-PBA did not significantly affect apoptosis on its own, its pretreatment markedly reduced the apoptosis caused by SSA treatment (**Figure 8A**). Subsequent Western blot analysis demonstrated

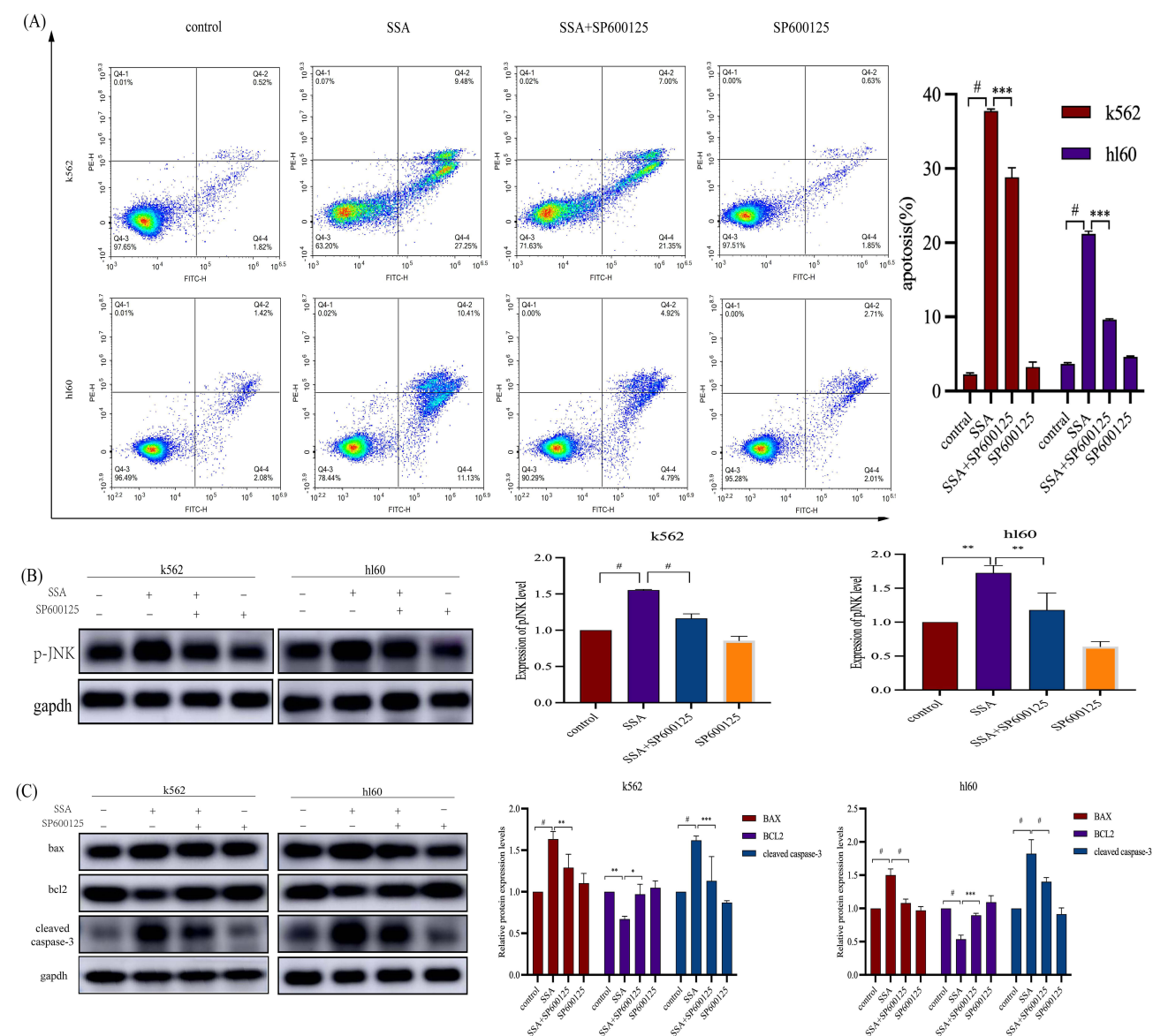


Figure 7 SSA-Induced Apoptosis is Mediated by the MAPK-p-JNK Signaling Pathway. **(A)** Flow cytometric analysis of apoptosis in AML cells treated with SP600125 (10 μ M, 2-hour pretreatment) and SSA (14 μ M, 24 hours), alone or in combination (K562/control: $2.26\% \pm 0.18\%$, SSA: $37.76\% \pm 0.25\%$, SSA+SP600125: $28.82\% \pm 1.305\%$, SP600125: $3.247\% \pm 0.67\%$, HL60/control: $3.64\% \pm 0.17\%$, SSA: $21.17\% \pm 0.37\%$, SSA+SP600125: $9.63\% \pm 0.11\%$, SP600125: $4.63\% \pm 0.08\%$) (n=5). **(B)** Western blot analysis of p-JNK protein expression in AML cells following treatment with SP600125 (10 μ M, 2-hour pretreatment) and SSA (14 μ M, 24 hours). GAPDH was used as a loading control (n=5). **(C)** Changes in the expression levels of cleaved caspase-3, Bax, and Bcl-2 in AML cells treated with SP600125 (10 μ M, 2-hour pretreatment) and SSA (14 μ M, 24 hours), individually or in combination. GAPDH served as a loading control (n=5). Significance is denoted as * $p < 0.05$, ** $p < 0.01$, *** $p < 0.001$, # $p < 0.0001$. The analysis was performed using GraphPad Prism software (version 9.0).

that 4-PBA pretreatment effectively counteracted the increased expression levels of ER stress-related proteins, including p-PERK/PERK, Bip, and CHOP, in SSA-treated K562 and HL60 cells. Additionally, 4-PBA markedly decreased the expression levels of MAPK-p-JNK proteins following SSA treatment (Figure 8B). Furthermore, 4-PBA administration led to a decrease in the levels of pro-apoptotic proteins, such as Bax and cleaved caspase-3, and an increase in the levels of the anti-apoptotic protein Bcl-2 in cells subjected to SSA (Figure 8C).

Together, these results suggest that SSA can trigger the apoptotic program in AML cells by activating the ERS signaling cascade response. These findings suggest that SSA can mediate the ERS-induced MAPK-p-JNK signaling pathway to promote AML cell apoptosis, which not only confirms the importance of ERS signaling in SSA-induced apoptosis of AML cells, but also reveals that 4-PBA, as an ERS inhibitor, can effectively intervene in SSA-induced apoptotic process.

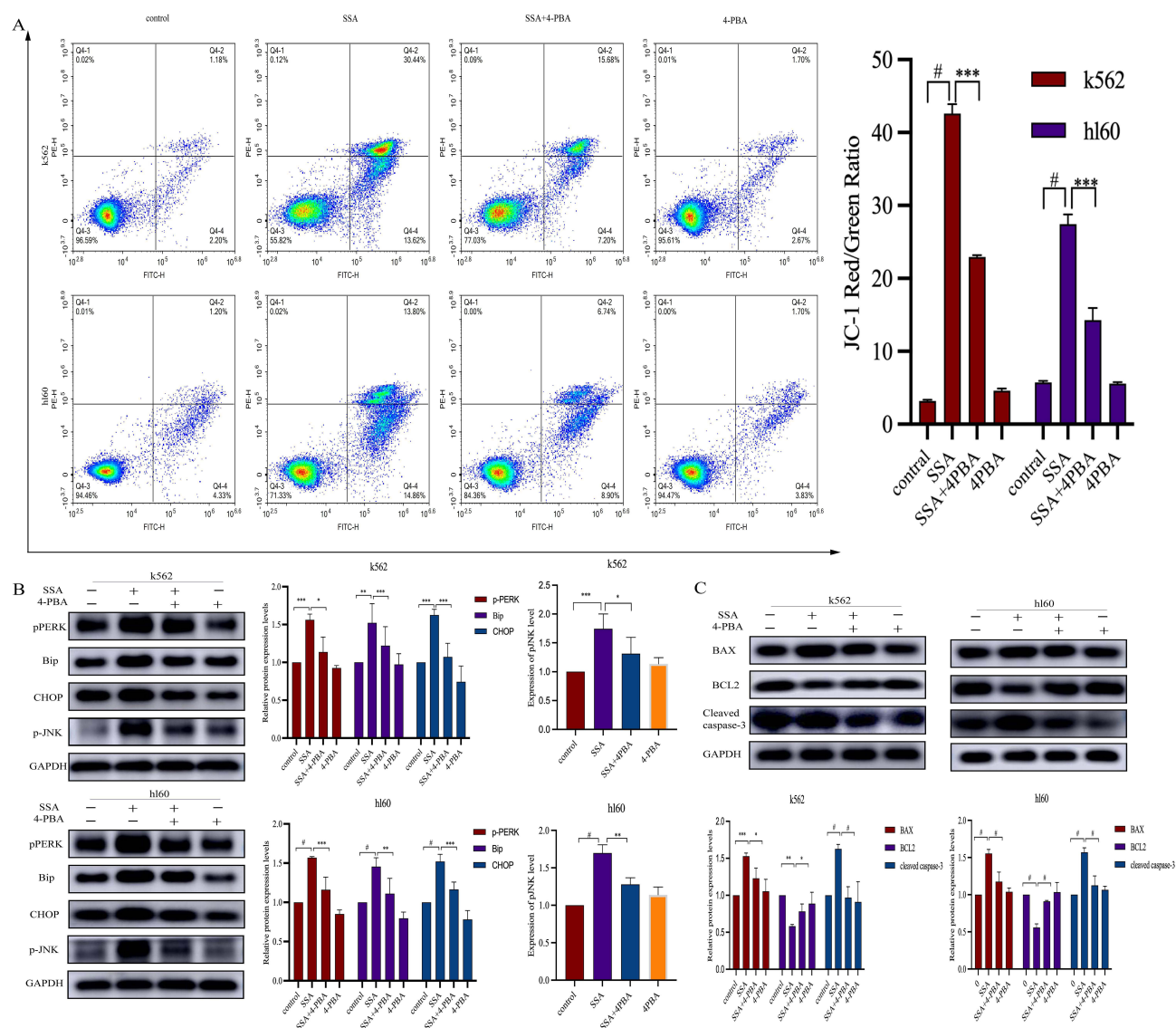


Figure 8 SSA induces apoptosis through the ERS-mediated p-JNK signaling pathway. **(A)** Flow cytometric analysis of apoptosis in K562 and HL60 cells treated with ER stress inhibitor 4-PBA (2h, 3mM) alone or in combination with SSA (14 μ M, 24 hours) (k562/control: 3.18% \pm 0.18%, SSA: 42.6% \pm 1.3%, SSA+4PBA: 22.9% \pm 0.27%, 4PBA: 4.62% \pm 0.26%, HL60/control: 5.72% \pm 0.21%, SSA: 27.43% \pm 1.34%, SSA+4PBA: 14.25% \pm 1.67%, 4PBA: 5.58% \pm 0.21%) (n=5). **(B)** Analysis of ER stress-associated proteins (pPERK/PERK, Bip, and CHOP) and p-JNK in AML cells following treatment with 4-PBA (2 hours, 3 mm) and SSA (24 hours, 14 μ M). GAPDH was used as an internal control (n=5). **(C)** Assessment of apoptosis-related proteins (BAX, BCL2, and cleaved caspase-3) in AML cells treated with 4-PBA (2 hours, 3 mm) and SSA (24 hours, 14 μ M). GAPDH served as an internal control (n=5). Significance is denoted as *p < 0.05, **p < 0.01, ***p < 0.001, #p < 0.0001. The analysis was performed using GraphPad Prism software (version 9.0).

Anti-Leukemic Effects of SSA in vivo

To assess the anti-AML effects of SSA in vivo, we established a NOD-SCID mouse xenograft tumor model using K562 and HL60 cell lines. In the K562 cohort, treatment with SSA at a concentration of 10 μ M resulted in a significant reduction in both tumor volume (Figure 9A, C and E) and tumor weight (Figure 9G) when compared to the control group. In the HL60 cohort, both low-dose and high-dose SSA groups demonstrated significant inhibition of tumor cell proliferation, as evidenced by substantial reductions in tumor volume (Figure 9B, D and F) and tumor weight (Figure 9H). Notably, the anti-AML effect was observed to be concentration-dependent.

To further investigate the in vitro mechanisms of SSA's anti-AML effects, we performed WB experiments on subcutaneous tumor tissues and found that, compared to the control group, SSA activated the ERS and p-JNK signaling

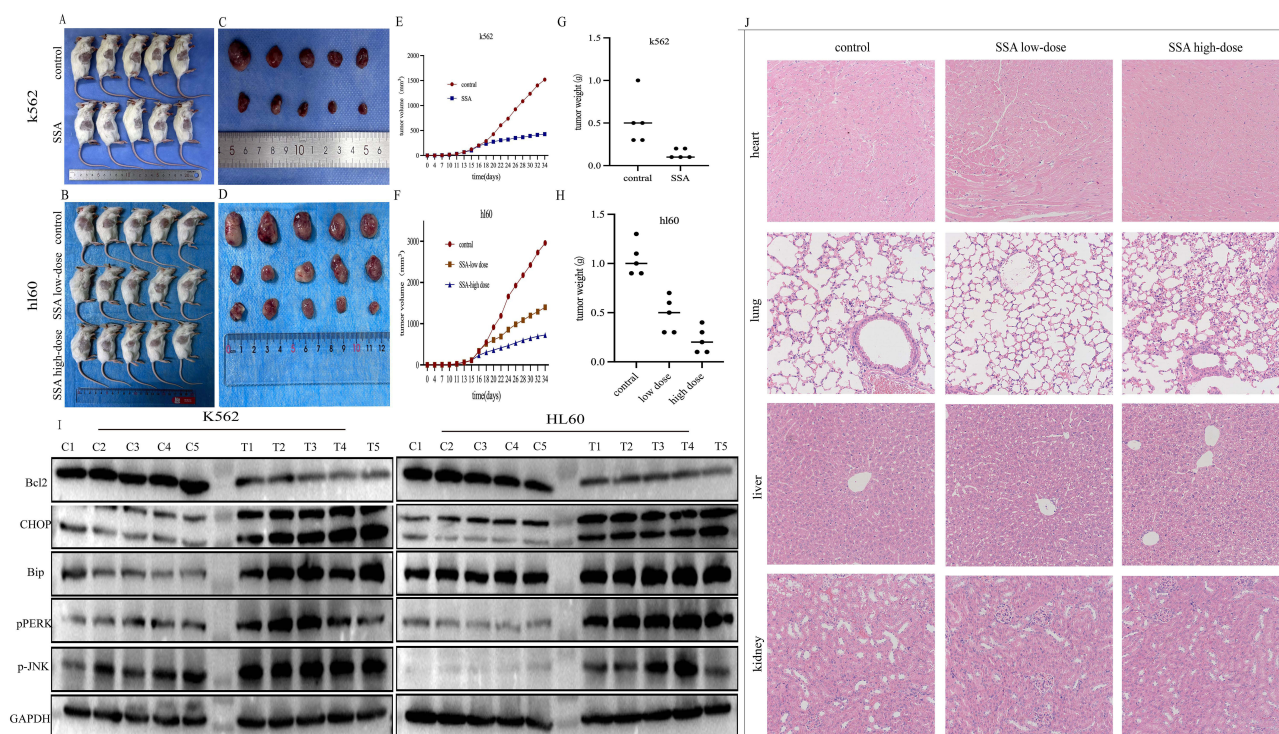


Figure 9 SSA suppresses the growth of AML xenografts in vivo. (A) K562 group rat images (n=5 for each group). (B) HL60 group rat images (n=5 for each group). (C) Tumor size in K562 group (n=5 for each group). (D) Tumor size in HL60 group (n=5 for each group). (E) Tumor volume over time in K562 group (n=5 for each group). (F) Tumor volume over time in HL60 group (n=5 for each group). (G) Tumor weight in K562 group (n=5 for each group). (H) Tumor weight in HL60 group (n=5 for each group). (I) Protein expression levels of BCL2, CHOP, Bip, pPERK, p-JNK in tumor tissues of control mice (C1, C2, C3, C4, C5) and treatment mice (T1, T2, T3, T4, T5). (J) HE staining was used to assess the histopathologic features of the heart, lungs, liver, and kidneys (n=5).

pathways and reduced the expression of the anti-apoptotic protein BCL2 (Figure 9I). These results suggest that SSA may inhibit AML cell proliferation and promote apoptosis by regulating these signaling pathways.

Histological examination of common organs in the HL60 group, using HE staining, revealed no substantial toxicity in either the low-dose or high-dose SSA treatment groups compared to the control group (Figure 9J). Collectively, these findings indicate that SSA effectively inhibits AML proliferation in vivo without eliciting significant toxicity.

Discussion

Clinical researchers are actively investigating novel therapeutic options for leukemia that offer a combination of high efficacy and low toxicity. Despite considerable research efforts, progress has been relatively modest, with only a limited number of new drugs receiving approval for the treatment of AML in recent years. In this context, naturally derived substances, particularly those commonly used as dietary supplements, have attracted growing interest for their potential antitumor properties. Plant-derived compounds, such as vincristine and etoposide, have shown significant therapeutic efficacy in hematologic malignancies and have been successfully incorporated into clinical practice as essential components of modern anti-leukemia treatment regimens.¹⁹ This progress highlights the rich bioactive resources found in nature and provides new hope and direction for the future treatment of AML and other hematologic malignancies.

SSA, the primary active ingredient derived from the traditional herb Chai Hu, has a chemical formula of $C_{42}H_{68}O_{13}$ and a relative molecular mass of 781 Da. It exhibits a melting point ranging from 224 to 230 °C and demonstrates favorable solubility characteristics in both water and alcohol.²⁰ Due to its substantial antitumor activity observed across various cancer models, SSA has gained recognition as a promising anticancer candidate with potential clinical applications.^{8,9,11} However, the specific biological effects of SSA on AML have not been adequately explored.

In this study, we elucidated the pathway through which SSA initiates mitochondrial apoptosis in AML cells via ERS. Importantly, we reveal for the first time the novel mechanism by which SSA induces apoptosis in AML cells through the

activation of the ERS-mediated JNK signaling pathway. The UPR signaling pathway, a crucial component of ERS, plays an essential role in maintaining cellular protein homeostasis and facilitating survival adaptations in cells under conditions of damage or stress.²¹ However, under conditions of prolonged or excessive ERS, the overproduction of ROS can lead to cellular dysfunction, ultimately culminating in apoptotic cell death.²²

In the context of ERS, the primary branch of the UPR, specifically the PERK-GRP78-CHOP axis, initiates a cascade of signaling events through the phosphorylation activity of the PERK kinase.²³ This signal transduction pathway culminates in the activation of cysteine asparaginase (Caspase) mediated by CHOP, thereby instigating the apoptotic process.²⁴ Recent literature further corroborates that excessive ERS can drive cells toward a terminal fate by activating a caspase-dependent apoptotic pathway.²⁵ Findings from Ki et al¹⁵ indicate that SSA inhibits apoptotic cell death by suppressing the PERK-ATF4-CHOP signaling axis, thereby suggesting a dual role of ERS in determining cellular fate. Consequently, delineating the interaction between SSA and ERS is crucial for elucidating the underlying mechanisms of its anti-tumor effects.

In the present study, we demonstrated that SSA activates the PERK-GRP78-CHOP axis, a pivotal branch of ERS, which in turn triggers the mitochondrial apoptotic pathway and accelerates the apoptotic process. Furthermore, the introduction of the ERS inhibitor 4-PBA resulted in a significant attenuation of SSA-induced apoptosis, underscoring the central role of ERS in mediating this apoptotic response. Although the pathways through which SSA induces apoptosis in AML cells have been initially outlined, the specific molecular mechanisms underlying these effects warrant further investigation.

Existing evidence indicates that the JNK signaling pathway can activate Caspase-9 and Caspase-3, thereby promoting apoptosis.²⁶ Prior studies have reported that Saikosaponin D (SSD), an isomer of SSA, inhibits proliferation and induces apoptosis in pancreatic cancer cells via activation of the JNK signaling pathway.²⁷ Given this research background, we hypothesized that SSA might regulate the apoptotic process in AML cells through a comparable mechanism involving the activation of the JNK signaling pathway. It is noteworthy that the JNK pathway constitutes one component of the MAPK signaling network, which encompasses three primary pathways: P38, ERK, and JNK.²⁸ Therefore, the present study aimed to investigate the specific branch of the MAPK signaling pathway through which SSA exerts its pro-apoptotic effects in AML cells.

Our results showed that SSA significantly increased the phosphorylation levels of p-JNK/JNK and pP38/P38 in AML cell lines, with a particularly marked upregulation of p-JNK/JNK. Additionally, we observed elevated expression of GRP78 and CHOP in the tumor tissues of SSA-treated mice, along with increased levels of JNK phosphorylation and the initiation of apoptosis, consistent with the results of our *in vitro* experiments. This phosphorylation event subsequently promoted apoptosis, thereby reinforcing the hypothesis that SSA modulates apoptosis in AML cells via the MAPK signaling pathway, while also providing nuanced insights into the potential mechanisms by which SSA may facilitate AML therapy, specifically highlighting the central role played by the JNK signaling pathway in this context. A substantial body of literature confirms that the JNK inhibitor SP600125 effectively inhibits apoptosis.^{29,30} In our experiments, SP600125 similarly demonstrated the capability to inhibit the pro-apoptotic effects of SSA in AML cells, an effect that coincided with alterations in the expression of proteins related to the mitochondrial apoptotic pathway. Collectively, these findings consistently affirm that SSA is efficacious in inducing apoptosis in AML cells.

Despite the significant pro-apoptotic effects of SSA observed in AML (up to 67.4% in K562 cells and 55.61% in HL60 cells at SSA concentrations up to 16 μ M), the biotoxicity of any compound must not be overlooked in clinical applications. The current standard therapy for AML, which typically involves a combination of anthracyclines and cytarabine, does provide some degree of efficacy,² however, its associated toxicities cannot be underestimated. High-dose cytarabine treatment, for instance, can lead to severe gastrointestinal and dermal toxicity, substantially increasing the risk of severe neutropenia, sepsis, and toxicity-related mortality.³¹ Literature reports indicate that at standard doses (usually 100 or 200 mg/m²), cytarabine can result in severe non-hematologic toxicity in 23%-61% of patients, with approximately 6%-16% of these cases evolving into fatal toxicity.³² Furthermore, cancer patients who undergo anthracycline-based chemotherapy face over a twofold increased risk of heart failure compared to those who do not receive such treatment.³³ These toxicities pose significant challenges, particularly for older patients or those unable to tolerate the adverse effects of conventional chemotherapeutic agents.

Our study demonstrated that SSA selectively inhibited the proliferation of AML cells while exhibiting minimal toxic effects on normal epithelial cells, including gastric epithelial cells (GES-1), renal tubular epithelial cells (HK-2), and urethral epithelial cells (SV-HUC-1). Similarly, we elucidated that SSA exerts antitumor effects *in vivo* while exhibiting minimal toxic effects on vital organs such as the heart, liver, kidneys, and lungs across both low and high dose concentration ranges. Immunosuppression and myelosuppression are common side effects of AML treatment, particularly with chemotherapeutic agents such as cytarabine, which can lead to severe leukopenia and thrombocytopenia.³⁴ However, studies have shown that SSA can enhance the body's anti-tumor immune response by regulating T cell function.³⁵ These findings suggest that SSA not only poses a lower risk of auto-immunosuppression and myelosuppression but may also exert immunomodulatory effects. Unfortunately, our study was unable to assess the role of SSA in relation to myelosuppression and immunosuppression in AML.

Moreover, it is noteworthy that SSA has demonstrated the ability to attenuate skin toxicity associated with chemotherapeutic agents and effectively alleviate cardiac dysfunction in models of anthracycline-induced heart failure.³⁶ Cardiotoxicity, particularly, remains a critical concern that warrants urgent attention within the realm of leukemia chemotherapy. Recent investigations have further corroborated that SSA presents no significant toxic effects on liver function and may aid in reducing acute liver injury induced by other pharmacological agents.³⁷

Although the metabolism of SSA in humans has not been extensively studied, traditional Chinese medicine (TCM) highlights the importance of oral administration of most herbs. This method necessitates consideration of the biotransformation of biologically active compounds, influenced by gastric acid and intestinal flora, in drug metabolism studies. In the late 1990s, several *in vitro* and *in vivo* studies demonstrated that, in gastric acid, SSA was completely converted to SSb1 in a 3:1 ratio over three hours, thereby facilitating absorption by the body.³⁸ Furthermore, SSA opens tight junctions between intestinal epithelial cells, which may enhance intestinal permeability and absorption. SSA can be excreted via the kidneys and bile, with extensive hepatic elimination through biliary excretion likely representing the major metabolic pathway for SSA.³⁹ Another study indicated that SSA is rapidly absorbed and eliminated in rats, showing low susceptibility to residues and accumulation, and it possesses a favorable safety profile.⁴⁰ Unfortunately, research on the intestinal absorption and metabolism of SSA—especially regarding the mechanisms involved in intestinal absorption and the enzymes related to its metabolism—has not been thorough enough.

Notably, AML is a heterogeneous disease characterized by multiple mutations and chromosomal abnormalities. These genetic variants not only define the different subtypes of the disease but also significantly impact treatment responsiveness and prognosis.⁴¹ Among these, the FLT3-ITD (internal tandem duplication) mutation is one of the most common genetic variants in adult AML and is strongly associated with poor prognosis. This mutation results in the sustained activation of the FLT3 receptor tyrosine kinase, which subsequently promotes cell proliferation and inhibits apoptosis.⁴² Research has shown that targeting the GRP78-ATF6-CHOP axis sensitizes AML to FLT3 inhibitors.⁴³ In contrast, SSA triggers apoptosis mediated by the JNK signaling pathway through the induction of ERS. This suggests that SSA may be particularly effective in selectively inducing stress in AML cells that are already under high oxidative stress due to FLT3-ITD mutations. Moreover, considering the critical role of the JNK signaling pathway in regulating cell survival and apoptosis, as well as its importance in responding to external stimuli such as oxidative stress, selective activation of this pathway by SSA may enhance its cytotoxic effects on FLT3-ITD-positive AML cells.

Evaluating the potential interactions of a new drug candidate with other medications is a crucial step in drug development. Studies have demonstrated that SSA synergistically enhances the sensitivity of gemcitabine in cholangiocarcinoma.⁴⁴ Additionally, the combination of SSA and adriamycin has been shown to be effective not only in treating breast cancer but also in reducing cardiotoxicity.⁴⁵ Unfortunately, our study did not assess the synergistic effects of SSA with commonly used drugs in AML. This will be a key focus of our future research.

In light of these findings, SSA emerges as a promising candidate for drug development in the treatment of AML, attributed to its favorable safety profile and potential for synergistic therapeutic effects when integrated into existing treatment regimens.

Conclusion

In the present study, we demonstrated that SSA significantly inhibited the proliferation of AML cell lines K562 and HL60 in a time- and concentration-dependent manner, inducing significant apoptosis at a concentration of 16 μ M (67.4% in K562 cells and 55.61% in HL60 cells). Additionally, transcriptome analysis revealed a significant enrichment of the MAPK signaling pathway following SSA treatment. Ex vivo experiments further confirmed that SSA promotes apoptosis in AML cells through the ERS-mediated MAPK-p-JNK signaling pathway.

Importantly, in the NOD-SCID mouse model, SSA not only significantly reduced tumor volume and weight but also did not cause significant toxicity to the liver, kidneys, lungs, or heart. These findings provide a strong molecular basis for considering SSA as a potential drug for the treatment of AML and open new avenues for research into its clinical application.

Future work, including necessary preclinical and clinical trials, will be crucial in validating the safety and efficacy of SSA in humans and advancing its translation to clinical practice.

Abbreviations

SSA, Saikosaponin A; AML, acute myeloid leukemia; ERS, endoplasmic reticulum stress; MAPK, Mitogen-Activated Protein Kinase; PERK, Protein kinase RNA-like endoplasmic reticulum kinase; UPR, Unfolded Protein Response; eIF2 α , Eukaryotic initiation factor 2 alpha; JNK, c-Jun N-terminal kinase; P-JNK, phosphorylation of c-Jun N-terminal kinase; CCK8, Cell Counting Kit 8 reagent; MMP, mitochondrial membrane potential; KEGG, Kyoto Encyclopedia of Genes and Genomes; GSEA, Gene Set Enrichment Analysis; p-ERK, phosphorylated Extracellular Signal-Regulated Kinase; p-PERK/PERK, Phosphorylated PKR-like ER Kinase; Bip, Binding Immunoglobulin Protein; CHOP, C/EBP Homologous Protein; 4-PBA, 4-phenylbutyric acid.

Data Sharing Statement

The datasets utilized and/or analyzed in this study can be obtained from the corresponding author upon reasonable request.

Ethical Approval

Our study adhered to the Declaration of Helsinki and ethical guidelines established by the Research Ethics Committee of the First Hospital of Lanzhou University. All clinical samples were collected with informed consent from the patients and the collection was approved the Research Ethics Committee of the First Hospital of Lanzhou University (LDYYLL2024-485).

We confirm that the use of the cell lines has been approved by the Research Ethics Committee of the First Hospital of Lanzhou University.

Acknowledgments

We would like to express my gratitude to the Laboratory of Clinical Molecular Cytogenetics and Immunology, the First Hospital of Lanzhou University for granting me access to their laboratory facilities.

Funding

This study was supported by Gansu Provincial Youth Science Foundation (23JRRA0951); Lanzhou Science and Technology Development Guiding Plan Project (2023-ZD-99); The First Hospital of Lanzhou University Youth Fund (ldyyyn2022-45).

Disclosure

The authors declare no competing interests.

References

1. Long Z-J, Wang J-D, Qiu S-X, et al. Dietary γ -mangostin triggers immunogenic cell death and activates cGAS signaling in acute myeloid leukemia. *Pharmacol Res.* 2023;197:106973. doi:10.1016/j.phrs.2023.106973

2. Senapati J, Kadia TM, Ravandi F. Maintenance therapy in acute myeloid leukemia: advances and controversies. *Haematologica*. 2023;108(9):2289–2304. doi:10.3324/haematol.2022.281810
3. Stoll JR, Battle L, Moy A, et al. Liposomal cytarabine and daunorubicin (CPX-351/Vyxeos)-associated distinct purpuric subtype of toxic erythema of chemotherapy: a retrospective review of 54 patients. *J Am Acad Dermatol*. 2022;86(1):232–234. doi:10.1016/j.jaad.2021.01.096
4. Wu T, Chen Z, Liu X, Wu X, Wang Z, Guo W. Targeting RSK2 in cancer therapy: a review of natural products. *Anticancer Agents Med Chem*. 2025;25(1):35–41. doi:10.2174/0118715206329546240830055233
5. Zhao ZX, Zou QY, Ma YH, et al. Recent progress on triterpenoid derivatives and their anticancer potential. *Phytochemistry*. 2025;229:114257. doi:10.1016/j.phytochem.2024.114257
6. Kang SJ, Lee YJ, Kim BM, et al. Effect of Bupleuri Radix extracts on the toxicity of 5-fluorouracil in HepG2 hepatoma cells and normal human lymphocytes. *Basic Clin Pharmacol Toxicol*. 2008;103(4):305–313. doi:10.1111/j.1742-7843.2008.00280.x
7. Zhao L, Jin L, Yang B. Saikosaponin A alleviates Staphylococcus aureus-induced mastitis in mice by inhibiting ferroptosis via SIRT1/Nrf2 pathway. *J Cell Mol Med*. 2023;27(22):3443–3450. doi:10.1111/jcmm.17914
8. Lan T, Wang W, Zeng XX, Tong YH, Mao ZJ, Wang SW. Saikosaponin A triggers cell ferroptosis in hepatocellular carcinoma by inducing endoplasmic reticulum stress-stimulated ATF3 expression. *Biochem Biophys Res Commun*. 2023;674:10–18. doi:10.1016/j.bbrc.2023.06.086
9. Wang C, Zhang R, Chen X, et al. The potential effect and mechanism of Saikosaponin A against gastric cancer. *BMC Complement Med Ther*. 2023;23(1):295.
10. Zhang Y, Dai K, Xu D, et al. Saikosaponin A alleviates glycolysis of breast cancer cells through repression of Akt/STAT3 pathway. *Chem Biol Drug Des*. 2023;102(1):115–125. doi:10.1111/cbdd.14259
11. Feng J, Xi Z, Jiang X, et al. Saikosaponin A enhances Docetaxel efficacy by selectively inducing death of dormant prostate cancer cells through excessive autophagy. *Cancer Lett*. 2023;554:216011.
12. Celik C, Lee SYT, Yap WS, Thibault G. Endoplasmic reticulum stress and lipids in health and diseases. *Prog Lipid Res*. 2023;89:101198. doi:10.1016/j.plipres.2022.101198
13. Alasiri G, Jiramongkol Y, Trakansuebkul S, et al. Reciprocal regulation between GCN2 (eIF2AK4) and PERK (eIF2AK3) through the JNK-FOXO3 axis to modulate cancer drug resistance and clonal survival. *mol Cell Endocrinol*. 2020;515:110932. doi:10.1016/j.mce.2020.110932
14. Deng Y, Li Y, Yang M, et al. Carfilzomib activates ER stress and JNK/p38 MAPK signaling to promote apoptosis in hepatocellular carcinoma cells. *Acta Biochim Biophys Sin*. 2024;56(5):697–708. doi:10.3724/abbs.2024040
15. Kim TW. Targeting ER stress with saikosaponin a to overcome resistance under radiation in gastric cancer cells. *Int J mol Sci*. 2023;24(6).
16. Du J, Song D, Cao T, et al. Saikosaponin-A induces apoptosis of cervical cancer through mitochondria- and endoplasmic reticulum stress-dependent pathway in vitro and in vivo: involvement of PI3K/AKT signaling pathway. *Cell Cycle*. 2021;20(21):2221–2232. doi:10.1080/15384101.2021.1974791
17. Xu Y, Wang X, Han D, et al. Revealing the mechanism of Jiegeng decoction attenuates bleomycin-induced pulmonary fibrosis via PI3K/Akt signaling pathway based on lipidomics and transcriptomics. *Phytomedicine*. 2022;102:154207. doi:10.1016/j.phymed.2022.154207
18. Subramanian A, Tamayo P, Mootha VK, et al. Gene set enrichment analysis: a knowledge-based approach for interpreting genome-wide expression profiles. *Proc Natl Acad Sci USA*. 2005;102(43):15545–15550. doi:10.1073/pnas.0506580102
19. Jiang X, Lin Y, Zhao M, et al. Platycodin D induces apoptotic cell death through PI3K/AKT and MAPK/ERK pathways and synergizes with venetoclax in acute myeloid leukemia. *Eur J Pharmacol*. 2023;956:175957. doi:10.1016/j.ejphar.2023.175957
20. Maccioni P, Chin Y-W, Corelli F, Kwon HC, Colombo G. Reducing effect of intragastrically administered saikosaponin A on alcohol and sucrose self-administration in rats. *Nat Prod Res*. 2023;37(24):4256–4260. doi:10.1080/14786419.2023.2177848
21. Heindryckx F, Sjöblom M. Endoplasmic reticulum stress in the pathogenesis of chemotherapy-induced mucositis: physiological mechanisms and therapeutic implications. *Acta Physiol*. 2024;240(8):e14188. doi:10.1111/apha.14188
22. Ketkar M, Desai S, Rana P, et al. Inhibition of PERK mediated UPR acts as a switch for reversal of residual senescence and as senolytic therapy in glioblastoma. *Neuro Oncol*. 2024;26(11):2027–2043. doi:10.1093/neuonc/noae134
23. Chen J, Fan W, Fan J, et al. Tetrahydrocurcumin attenuates polymyxin B sulfate-induced HK-2 cells apoptosis by inhibiting endoplasmic reticulum stress-mediated PERK / eIF2α / ATF4 / CHOP signaling pathway axis. *Environ Toxicol: Int J*. 2024;39(11):4995–5007. doi:10.1002/tox.24376
24. Wu S, Wang B, Li H, et al. Targeting STING elicits GSDMD-dependent pyroptosis and boosts anti-tumor immunity in renal cell carcinoma. *Oncogene*. 2024;43(20):1534–1548. doi:10.1038/s41388-024-03013-4
25. Zhou D, Yin M, Kang B, et al. CCT020312 exerts anti-prostate cancer effect by inducing G1 cell cycle arrest, apoptosis and autophagy through activation of PERK/eIF2α/ATF4/CHOP signaling. *Biochem Pharmacol*. 2024;221:116038. doi:10.1016/j.bcp.2024.116038
26. Farrell L, Puig-Barbe A, Haque MI, et al. Actin remodeling mediates ROS production and JNK activation to drive apoptosis-induced proliferation. *PLoS Genet*. 2022;18(12):e1010533. doi:10.1371/journal.pgen.1010533
27. Lai M, Ge Y, Chen M, Sun S, Chen J, Cheng R. Saikosaponin d inhibits proliferation and promotes apoptosis through activation of MKK4-JNK signaling pathway in pancreatic cancer cells. *Onco Targets Ther*. 2020;13:9465–9479. doi:10.2147/OTT.S263322
28. Lee S, Rauch J, Kolch W. Targeting MAPK signaling in cancer: mechanisms of drug resistance and sensitivity. *Int J mol Sci*. 2020;21(3).
29. Xie L, Liang S, Jiwa H, et al. Securinine inhibits the tumor growth of human bladder cancer cells by suppressing Wnt/β-catenin signaling pathway and activating p38 and JNK signaling pathways. *Biochem Pharmacol*. 2024;223:116125. doi:10.1016/j.bcp.2024.116125
30. Feng Q, Hu K, Hu H, et al. Berberine derivative DCZ0358 induce oxidative damage by ROS-mediated JNK signaling in DLBCL cells. *Int Immunopharmacol*. 2023;125(Pt A):111139. doi:10.1016/j.intimp.2023.111139
31. Bradstock KF, Link E, Collins M, et al. A randomized trial of prophylactic palifermin on gastrointestinal toxicity after intensive induction therapy for acute myeloid leukaemia. *Br J Haematol*. 2014;167(5):618–625. doi:10.1111/bjh.13086
32. Fanciullino R, Farnault L, Donnette M, et al. CDA as a predictive marker for life-threatening toxicities in patients with AML treated with cytarabine. *Blood Adv*. 2018;2(5):462–469. doi:10.1182/bloodadvances.2017014126
33. Qiao X, van der Zanden SY, Li X, et al. Diversifying the anthracycline class of anti-cancer drugs identifies aclarubicin for superior survival of acute myeloid leukemia patients. *mol Cancer*. 2024;23(1):120. doi:10.1186/s12943-024-02034-7
34. Drenberg CD, Hu S, Li L, et al. ABCC4 is a determinant of cytarabine-induced cytotoxicity and myelosuppression. *Clin Transl Sci*. 2016;9(1):51–59. doi:10.1111/cts.12366

35. Sun Y, Cai TT, Zhou XB, Xu Q. Saikosaponin a inhibits the proliferation and activation of T cells through cell cycle arrest and induction of apoptosis. *Int Immunopharmacol.* **2009**;9(7–8):978–983. doi:10.1016/j.intimp.2009.04.006
36. Huang C, Qiu S, Fan X, et al. Evaluation of the effect of Shengxian decoction on doxorubicin-induced chronic heart failure model rats and a multicomponent comparative pharmacokinetic study after oral administration in normal and model rats. *Biomed Pharmacother.* **2021**;144:112354. doi:10.1016/j.biopha.2021.112354
37. Wu S-J, Lin Y-H, Chu -C-C, Tsai Y-H, Chao JCJ. Curcumin or saikosaponin a improves hepatic antioxidant capacity and protects against CCl4-induced liver injury in rats. *J Med Food.* **2008**;11(2):224–229. doi:10.1089/jmf.2007.555
38. Shimizu K, Amagaya S, Ogihara Y. Structural transformation of saikosaponins by gastric juice and intestinal flora. *J Pharmacobiodyn.* **1985**;8(9):718–725. doi:10.1248/bpb1978.8.718
39. Fu R, Liu J, Xue Y, Zhang Z, Song R. Effects of animal strain, dose, and cotreatment with saikosaponin b(2) on the pharmacokinetics of Saikosaponin a in rats. *Eur J Drug Metab Pharmacokinet.* **2019**;44(6):827–836. doi:10.1007/s13318-019-00569-5
40. Yin P, Han X, Yu L, et al. Pharmacokinetic analysis for simultaneous quantification of Saikosaponin A- paeoniflorin in normal and poststroke depression rats: a comparative study. *J Pharm Biomed Anal.* **2023**;233:115485. doi:10.1016/j.jpba.2023.115485
41. Kivioja J, Malani D, Kumar A, et al. FLT3-ITD allelic ratio and HLF expression predict FLT3 inhibitor efficacy in adult AML. *Sci Rep.* **2021**;11(1):23565. doi:10.1038/s41598-021-03010-7
42. Long J, Chen X, Shen Y, et al. A combinatorial therapeutic approach to enhance FLT3-ITD AML treatment. *Cell Rep Med.* **2023**;4(11):101286. doi:10.1016/j.xcrm.2023.101286
43. Sun X, Li Y, Du J, et al. Targeting ceramide transfer protein sensitizes AML to FLT3 inhibitors via a GRP78-ATF6-CHOP axis. *Nat Commun.* **2025**;16(1):1358. doi:10.1038/s41467-025-56520-7
44. Song F, Wang CG, Wang TL, et al. Enhancement of gemcitabine sensitivity in intrahepatic cholangiocarcinoma through Saikosaponin-a mediated modulation of the p-AKT/BCL-6/ABCA1 axis. *Phytomedicine.* **2024**;133:155944. doi:10.1016/j.phymed.2024.155944
45. Li D, Yao Y, Wang K, et al. Targeted delivery of Saikosaponin A and doxorubicin via hyaluronic acid-modified ZIF-8 nanoparticles for TNBC treatment: inhibiting metastasis and reducing cardiotoxicity. *Biomater Adv.* **2025**;167:214114. doi:10.1016/j.bioadv.2024.214114

Drug Design, Development and Therapy

Dovepress
Taylor & Francis Group

Publish your work in this journal

Drug Design, Development and Therapy is an international, peer-reviewed open-access journal that spans the spectrum of drug design and development through to clinical applications. Clinical outcomes, patient safety, and programs for the development and effective, safe, and sustained use of medicines are a feature of the journal, which has also been accepted for indexing on PubMed Central. The manuscript management system is completely online and includes a very quick and fair peer-review system, which is all easy to use. Visit <http://www.dovepress.com/testimonials.php> to read real quotes from published authors.

Submit your manuscript here: <https://www.dovepress.com/drug-design-development-and-therapy-journal>